



ISSN: 2508-7894

KJAI website: <http://accesson.kr/kjai>doi: <http://doi.org/10.24225/kjai.2024.12.3.9>

# AR Marker Detection Technique-Based Autonomous Attitude Control for a non-GPS Aided Quadcopter

Yeonwoo LEE<sup>1</sup>, Sun-Kyoung KANG<sup>2</sup>

Received: June 02, 2024. Revised: July 17, 2024. Accepted: September 05, 2024.

## Abstract

This paper addresses the critical need for quadcopters in GPS-denied indoor environments by proposing a novel attitude control mechanism that enables autonomous navigation without external guidance. Utilizing AR marker detection integrated with a dual PID controller algorithm, this system ensures accurate maneuvering and positioning of the quadcopter by compensating for the absence of GPS, a common limitation in indoor settings. This capability is paramount in environments where traditional navigation aids are ineffective, necessitating the use of quadcopters equipped with advanced sensors and control systems. The actual position and location of the quadcopter is achieved by AR marker detection technique with the image processing system. Moreover, in order to enhance the reliability of the attitude PID control, the dual closed loop control feedback PID control with dual update periods is suggested. With AR marker detection technique and autonomous attitude control, the proposed quadcopter system decreases the need of additional sensor and manual manipulation. The experimental results are demonstrated that the quadrotor's autonomous attitude control and operation with the dual closed loop control feedback PID controller with hierarchical (inner-loop and outer-loop) command update period is successfully performed under the non-GPS aided indoor environment and it enhanced the reliability of the attitude and the position PID controllers within 17 seconds. Therefore, it is concluded that the proposed attitude control mechanism is very suitable to GPS-denied indoor environments, which enables a quadcopter to autonomously navigate and hover without external guidance or control.

**Keywords :** AR marker, Attitude control algorithm, Image processing, GPS, Quadcopter

**Major Classification Code:** Artificial Intelligence, etc

## 1. Introduction

With the popularity of Unmanned Aerial Vehicles (UAVs), a quadrotor has received significant attention in recent research works. Although a variety of flight control researches with results and applications have received significant attention, it is still considered an open issue to be discussed. Flight control of quadcopter requires highly delicate sensory data acquisition, processing and computing

load in order to maneuver the rotor propeller of a quadcopter. The major functions of an autopilot UAV are stabilization, control, and way-point navigation with flight controllers, which are capable of overcoming the changes in the payload and the circumstance and providing the optimal flight trajectory with tolerable faults and errors. This issue is considered as a challenging problem because the fly dynamics of the quadcopter is complex with high nonlinearities (Mian & Wang, 2008).

1 First Author. Professor, Department of Artificial Intelligence Engineering, Mokpo National University, Korea. Email: [ylee@mokpo.ac.kr](mailto:ylee@mokpo.ac.kr)

2 Corresponding Author. Professor, Department of Computer Engineering, Wonkwang University, Korea. Email: [doctor10@wku.ac.kr](mailto:doctor10@wku.ac.kr)

© Copyright: The Author(s)

This is an Open Access article distributed under the terms of the Creative Commons Attribution Non-Commercial License (<http://creativecommons.org/licenses/by-nc/4.0/>) which permits unrestricted noncommercial use, distribution, and reproduction in any medium, provided the original work is properly cited.

A quadcopter with four rotor propellers follows the fly dynamic equations of attitude (roll, pitch, and yaw) and translation position (altitude) motions in 3-dimensional space, which are controlled by adjusting the angular speeds (inputs) of four propeller (Salih et al., 2010). The fly dynamic of the translation motion can be derived Newton-Euler formulation (Elruby et al., 2012) and Lagrange-Euler formulation (Gheorghita et al., 2015), while the rotational movement mechanics of a quadcopter can be derived by Euler approach. Hence, with the dynamic model, the flight control strategy can improve the performance of the quadcopter.

The generally well-known three types of flight control strategies are linear flight control, nonlinear flight control, and learning based flight control system (Cai et al., 2014). The most commonly used linear flight control strategies are the proportional derivative (PD) control (Nemati & Kumar, 2014), the proportional integral derivative (PID) control (Goel et al., 2009), the fuzzy based PID control (Razinkova et al., 2014; Seidabad et al., 2014), and linear quadratic gaussian (LQG) (Tahir et al., 2016), etc. The modeling of the fly dynamics and the attitude-altitude control algorithm of quadcopter have been widely studied by many researchers.

Among those strategies, the PID feedback linearization has demonstrated exceptional performance of decoupling the quadcopter attitude mode with precision and agility in many circumstances. It is noted that a PID controller guarantees ideal performance in a stale environment. However, with the unknown dynamics such as wind and variable payloads, it is far from optimal operation. Thus, the flight control strategy for the quadcopter needs an intelligent devise with agile adaptability to unexpectable dynamics and environment. It should be noted that most of those researches are mainly based on aid of the external measurement such as GPS and motion capture systems for localizing and obtaining state information of the UAVs. In general, most UAVs, i.e., quadcopter, utilize the GPS-aided location information given by GPS for delivering a precise navigation performance. Moreover, GPS-aided UAV system still needs the precise and well-trained skill of manipulation of the quadcopter for controlling and hovering aerial vehicle under the unexpected circumstance such as inaccurate inertia sensor detection and slip in aerial space. In indoor environments, this drawback becomes more severe since it cannot use a help of GPS for guiding a quadcopter (Achtelik et al., 2009). Thus, this results in the need of an intelligent autonomous flight control mechanism.

In indoor environments, the deployment of quadcopters is essential due to their ability to facilitate detailed inspections, enhance inventory management, support emergency responses, contribute to media production, aid in research and development, and potentially revolutionize

internal delivery systems. Moreover, the unique capabilities of quadcopters, such as vertical takeoff and landing, precise maneuverability, and compact design, render them indispensable for executing tasks in complex indoor settings where traditional methods may be inefficient or infeasible.

In this paper, therefore, we propose the fly control strategy with the autonomous attitude control algorithm and stabilizing operation of a quadcopter in a GPS-denied indoor environment. For autonomous attitude control, this paper proposes the dual closed control loop feedback PID control mechanism for enhancing the performance, which is modified and enhanced version of the conventional PID control scheme. Moreover, for detection of the exact position, a simple and efficient technique is suggested in this paper, i.e., AR marker detection technique with image processing. With these two techniques, the quadcopter can maneuver and hover without a GPS location service, and the additional sensory parts/devices in a quadcopter are not necessary by virtue of the autonomous flight control. We demonstrate the experimental test and results of the quadrotor's autonomous attitude control and operation under the non-GPS aided indoor environment. This paper is organized as following sections. In Section 2, the fly dynamics of quadcopter and its attitude control algorithm are described. In Section 3, the proposed AR-marker based attitude control algorithm is presented. In Section 4, AR marker detection technique, non-GPS aided quadcopter tested, and experimental results are shown followed by conclusion in Section 5.

## 2. Quadcopter Fly Dynamics and Its Attitude Control Algorithm

### 2.1. Structure and Fly Dynamics of Quadcopter

A quadcopter generally has two pairs of rotor propellers places in respectively opposite position. Each pair of rotor propellers will spin in the same direction, and side-by-side rotor will spin oppositely. Flight dynamic movement is controlled by these four rotors' spinning movement and their angular velocities. A dynamic movement with force and moment can lead to pitch, roll, yaw or list rotation moment inertia. Thus, a quadcopter attitude is a kind of an aircraft with six degrees of freedom (DOF), i.e., three angular (rotational) positions of the quadcopter's body and three linear (translational) position in an Earth inertial frame. All DOFs are covered by the linear and angular orientation vectors of the quadcopter.

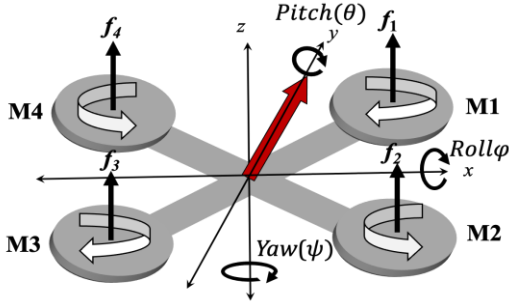


**Figure 1:** The illustrated structure of a quadcopter schematic and its rotation movement; pitch, roll, yaw angles.

It can be seen that with four control inputs from the rotor propelled (one to each motor), there are six state outputs of the quadcopter fly dynamic. This result requires an onboard computer monitoring and computing motor signals to maintain a stable flight of quadcopter. Figure 1 shows the structure of a quadcopter schematic and its rotation movements. We indicate with  $M_i, i \in \{1, 2, \dots, K\}$  where  $K$  is the total number of motors for a quadcopter.

## 2.2. Mathematical Modelling

In this research, we use four rotor propellers, i.e.,  $\{M_1, M_2, M_3, M_4\}$ . As shown in Fig. 1, each rotation movement angles based on Newton-Euler equation model can be modelled as  $\varphi, \theta, \psi$ . Each angle represents roll, pitch, and yaw rotation in 3-dimensions. We indicate rotation around x-axis as roll ( $\varphi$ ) movement, rotation around y-axis as pitch ( $\theta$ ) movement, and rotation around z-axis as yaw ( $\psi$ ) movement. Then, Moreover, these four rotors produce a certain amount of upward thrust, indicated with  $\{f_1, f_2, f_3, f_4\}$  for each rotor.

Based on Newton-Euler kinematics modeling [3], four rotors deliver a certain amount of lift up forces  $\{f_1, f_2, f_3, f_4\}$  for each rotor  $M_i$  with respect to Earth inertial frame axes such as x-axis, y-axis and z-axis. Thus, the orientation of the rotor's body frame axes results in change of angular movement on roll ( $R_x$ ), pitch ( $R_y$ ), and yaw ( $R_z$ ). Based on the kinematic movement frame theory and Euler-Lagrange derivation (Gheorghita et al. (2015), the angular motion matrices on each axis can be written in Eq. (1) as a form of transformation 3x3 matrices, and the overall rotation movement ( $R_{xyz}$ ) of the body frame can be given in Eq. (2).

$$R_x = \begin{bmatrix} 1 & 0 & 0 \\ 0 & \cos\varphi & -\sin\varphi \\ 0 & \sin\varphi & \cos\varphi \end{bmatrix}; R_y = \begin{bmatrix} \cos\theta & 0 & \sin\theta \\ 0 & 1 & 0 \\ -\sin\theta & 0 & \cos\theta \end{bmatrix};$$

$$R_z = \begin{bmatrix} \cos\psi & -\sin\psi & 0 \\ \sin\psi & \cos\psi & 0 \\ 0 & 0 & 1 \end{bmatrix} \quad (1)$$

$$R_{xyz} = R_x R_y R_z \quad (2)$$

Then, these linear ( $x, y, z$ ) and angular motion (angles of  $\varphi, \theta, \psi$ ) can be rewritten as following:

$$\xi = [xyz]^T, \eta = [\varphi\theta\psi]^T, q = [xyz\varphi\theta\psi] \quad (3)$$

where  $\xi$  is the state of translational motion movement,  $\eta$  is a rotational movement, and  $q$  is the combination of these two parameters. Based on Euler-Lagrange equation, each movement can be written as in Eq. (4).

$$L(q, \dot{q}) = T_{trans} + T_{rotor} - U; \\ L(q, \dot{q}) = \frac{1}{2} m \dot{\xi}^T \dot{\xi} + \frac{1}{2} J \dot{\eta}^T \dot{\eta} - mgz \quad (4)$$

where  $T_{trans}$  is a torque of translational motion movement and  $T_{rotor}$  is a torque of rotational movement,  $\tau$  is the external torque applied to the body frame,  $m$  is the mass of the quadcopter and  $g$  is the gravity velocity. According to second law of Newton for translation motion, the angular rate measured by quadcopter sensor ( $F_\xi$ ) can be given by substituting parameters of Eq. (3) into Eq. (4) as following:

$$F_\xi = m \ddot{\xi} + [0 \ 0 \ mg]^T = R_{xyz}^T [0 \ 0 \ u]^T \\ = [-u \sin\theta \ u \cos\theta \sin\varphi \ u \cos\theta \cos\varphi]^T \quad (5)$$

where  $u$  is the total thrust produced by the four propellers of the quadcopter ( $u = (f_1 + f_2 + f_3 + f_4)/m$ ). Thus, from the Eq. (5), we can get the translational motion (control input,  $\ddot{\xi} = [\ddot{x} \ \ddot{y} \ \ddot{z}]^T$ ) as following:

$$\ddot{x} = -u \sin\theta, \ddot{y} = u \cos\theta \sin\varphi, \ddot{z} = u \cos\theta \cos\varphi - g \quad (6)$$

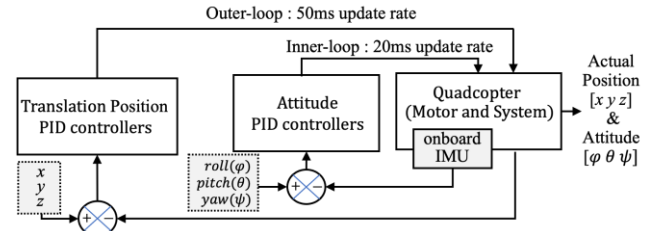


**Figure 2:** Quadcopter control system with the hierarchical closed control loop feedback PID controller

According to Euler's law for rotational motion, the external rotational torque equation on the body frame can be rewritten as shown in Eq. (7).

$$\tau = J \ddot{\eta} = J [\ddot{\varphi} \ \ddot{\theta} \ \ddot{\psi}]^T \cong [\tau_\varphi \ \tau_\theta \ \tau_\psi]^T; \\ \tau_\varphi = l(f_4 - f_2), \tau_\theta = l(f_3 - f_1), \tau_\psi = \sum_{i=1}^4 \tau_{M_i} \quad (7)$$

where  $\tau_{M_i}$  is the moments for each rotor, and  $l$  is the distance between the rotor and the center of a quadcopter.

### 3. Proposed AR-Marker-Based Attitude Control Algorithm

#### 3.1. Attitude PID Controller

The closed loop feedback PID control system for the quadcopter in hovering movement is generally used for achieving stability. In this study, we have six PID controllers of each axis and rotations,  $x$ ,  $y$ ,  $z$ -axis, roll, pitch and yaw. The proposed quadcopter attitude control algorithm is mainly based on managing hierarchical PID controllers by autonomously adjusting the position ( $x$ ,  $y$ ,  $z$ ) and the attitude (angles of  $\varphi$ ,  $\theta$ ,  $\psi$ ) of the quadcopter. Figure 2 shows the quadcopter control system with double closed loop feedback PID controller.

Meanwhile each controller of  $x$ -axis and  $y$ -axis translation position controls each adjustment of angular alternation on each axis, the controller of  $z$ -axis is handled by the overall averaged thrust by four rotors. Each translation position is controlled and updated by feedback data after image processing of RGB camera-based AR marker detection. This PID controller is shown in Fig. 2 as *the translation position PID controller*. This outer-loop update period of the translation position of the quadcopter body frame is every 50ms. In *the attitude PID controller* in Fig. 2, this inner-loop process of control, adjustment and correction is carried out with translation position data and angular (rotation) movement data by every 20ms update period. Note that the outer-loop update rate of translation position is 50ms period, and the inner-loop update rate of angular movement (attitude control) is 20ms period. It should be noticed that this two closed control loop feedback PID control mechanism plays essential role in controlling and stabilizing the attitude PID controllers of the quadcopter system.

The attitude PID controllers are linear feedback controllers expressed as

$$u(t) = K_p e(t) + K_i \int_0^t e(\tau) d\tau + K_d \frac{de(t)}{dt} \quad (8)$$

$$e(t) = X_d(t) - X(t) \quad (9)$$

where  $u(t)$  is the control output signal and  $K_p, K_i, K_d$  are the proportional, integral, and derivative gains, respectively. In Eq. (9),  $e(t)$  is the difference between the desired state  $X_d(t)$  and the actual state  $X(t)$ . The torques generated by the rotors on  $x$ -axis or  $y$ -axis may produce in change in pitch and roll angles. In modeling of PID controllers in Eq. (8) and (9),  $K_i$  is generally used as a configurable parameter for reducing the final error of the

system, and just two  $K_p$  and  $K_i$  are considered as control parameters.

#### 3.2. Attitude Control Parameter and Simulation Modelling

With a translational position vector ( $p = [x \ y \ z]^T$ ), the translational velocity ( $v = [v_x \ v_y \ v_z]^T$ ) can be derived by Newton-Euler kinetic model. Recalling Eq. (6) and the relation equation with respect to the torque ( $T$ ) and the angular velocity ( $\omega$ ), i.e.,  $T = J\dot{\omega} + \omega \times J\omega$  where  $\omega = C\dot{\eta}$ , we can derive the related equation as  $T_d = JC\dot{\eta}$ . The translational torque ( $T_{trans}$ ) can be produced by the angular speed of propellers about  $x$ -axis,  $y$ -axis, and  $z$ -axis. Then, translational torque will be influenced by the moments of inertia, which can be calculated as following:

$$T_{trans} = \begin{bmatrix} \tau_x \\ \tau_y \\ \tau_z \end{bmatrix} = \begin{bmatrix} l(f_2 - f_4) \\ l(f_3 - f_1) \\ r(f_1 - f_2 + f_3 - f_4) \end{bmatrix} \quad (10)$$

where  $l$  is the distance between quadcopter rotor and centroid,  $r$  is the correlation coefficients of torques and moments. It is noted that the nominal coefficients of PID for the stability equation are based on the angular velocity equation of the quadcopter (Elruby et al., 2012; Gheorghita et al., 2015). Thus, based on Eq. (6), Eq. (7) and Eq. (10), the PID controller in translational position can be given in Eq. (11).

$$\begin{bmatrix} \tau_x \\ \tau_y \end{bmatrix} = \begin{bmatrix} K_{p,\phi}(\ddot{\phi}_p - \ddot{\phi}) + K_{d,\phi}(\dot{\phi}_d - \dot{\phi})I_{xx} \\ K_{p,\theta}(\ddot{\theta}_p - \ddot{\theta}) + K_{d,\theta}(\dot{\theta}_d - \dot{\theta})I_{yy} \end{bmatrix} \quad (11)$$

where  $I_{xx}$  and  $I_{yy}$  are the moments of inertia matrices.

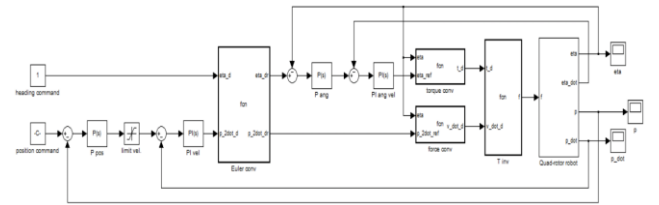


**Figure 3:** The simulink attitude control function block within an onboard DSP software unit of the quadcopter in Fig. 2

Moreover, the derivative of the translational velocity ( $\dot{v}_d$ ) can be approximated as

$$\dot{v}_d \approx R^{-1} \ddot{p}_{ref} \quad (12)$$

Based on equations from Eq. (10) to Eq. (12), the attitude control function block is implemented by Matlab simulink block as shown in Fig. 3.

## 4. AR Marker Detection and Non-GPS Aided Quadcopter Test-Bed

### 4.1. Image Processing-based AR Marker Detection

The marker detection technique is quite generally used to detect the exact location or position of the target in applications of the augmented reality (AR) (Quach et al., 2018; Qi et al., 2018). In this study, two color (green and red) AR markers attached on the body of a quadcopter are considered as depicted in Fig. 4, since the rationale behind this choice is that two AR markers are both sufficient and essential. A single AR marker limits the ability to accurately establish the quadcopter's position and orientation, while using three or four AR markers might improve performance, the enhancement is not significantly impactful, thus this approach primarily considers the worst-case scenario. Some specifically designed markers are installed on the body, and a RGB camera facing downward is attached on the ceiling in the indoor environment for capturing images of two AR markers on a quadcopter.



**Figure 4:** A quadcopter with attached two (green and red colored) AR markers on the frame body

These recorded images are mainly RGB color information and these are used to distinguish the position of a quadcopter. The recorded RGB images are converted to binary images and transformed into each gain coefficient of the green-color and red-color marker such  $R_{im}$  and  $G_{im}$ , respectively. Note that each color pixel of the RGB image has a certain color level of 0~255. Hence, only if the following conditional equation of Eq. (13) is satisfied, the detected AR marker could be successfully recognized as a useful marker.

$$\begin{aligned} R_{im}^i &: R_{im} > K_{RR}^i R_{im} + K_{RG}^i G_{im} + R_{th}^i \quad \text{and} \\ G_{im}^i &: G_{im} > K_{GR}^i R_{im} + K_{GG}^i G_{im} + G_{th}^i \end{aligned} \quad (13)$$

where  $R_{th}^i$  and  $G_{th}^i$  are threshold values of red and green color gain coefficients and  $K_{RR}^i$ ,  $K_{RG}^i$ ,  $K_{GR}^i$ ,  $K_{GG}^i$  are configurable coefficients depending on the physical variance of the color marker. With this conditional equation, the reliability of the detected AR marker color data is guaranteed and the possible detection error caused by the unexpected variables such as a sudden altitude change or an attitude change of a quadcopter could be compensated. Moreover, other additive noise problem occurred beyond scope of the AR color marker detection can be tackled down by applying image processing techniques such as erosion and dilation methods.

### 4.2. Experimental Test-bed and Results

In this paper, the autonomous attitude control mechanism with RGB camera adopted AR marker detection and image processing technique is proposed for providing sustainable stability of the non-GPS aided quadcopter. Thus, this enables a quadcopter to autonomously navigate and hovering without external guidance or control in the GPS-denied indoor environment. This test-bed for a non-GPS aided quadcopter with a RGB camera on the ceiling is illustrated in Fig. 4.

The experimental setup is illustrated in Fig. 5 where the system block diagram for a non-GPS aided quadcopter test-bed is shown. This test-bed setup demonstrates how the quadcopter and its peripherals work. The RGB camera-based image processing station on the ceiling generates  $[x, y, z]$  data after AR-marker detection and noise reduction image processing, and this data is transmitted to the quadcopter by Bluetooth communication link. In the quadcopter, DSP block with the TMS320F38335 (32-bit microcontrollers optimized for processing and sensing processing and actuation in real-time control applications) performs functions of the translational PID controllers and the attitude PID controllers with the received data from the image processing system on the ceiling. For adjusting these PID controllers, the IMU block delivers the attitude data (angles of  $\phi$ ,  $\theta$ ,  $\psi$ ) to the PID controllers in order to control attitude of the quadcopter. Then, outputs of the PID controllers are transmitted to motor transmission blocks and brushless direct current motor (BLDC) motors. By successful operations of such DPS and IMU functional blocks, the hierarchical closed control loop feedback PID controllers in Fig. 2 are in an autonomous attitude control mode of operation for controlling and stabilizing a quadcopter.

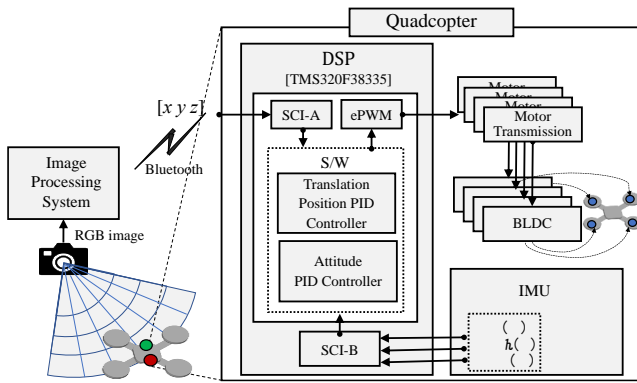
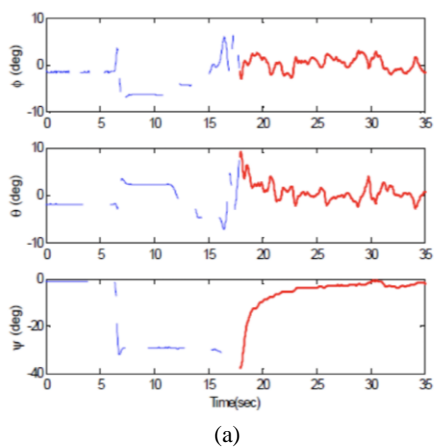
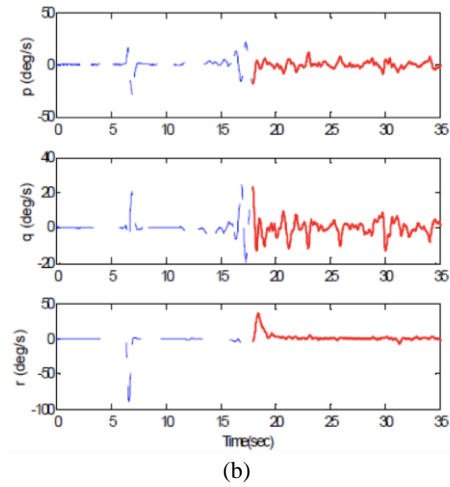


**Figure 5:** Functional block diagram of the non-GPS aided quadcopter and a RGB camera-adopted image processing station

The experimental test for demonstrating the quadrotor’s autonomous attitude control and operation in hovering flight under the real non-GPS aided indoor environment is carried out. The experimental results for tracking data of three angular (rotational) positions of the quadcopter’s body ( $\phi, \theta, \psi$ , in [deg]) and three angular rates ( $p = \dot{\phi}, q = \dot{\theta}$ , and  $r = \dot{\psi}$ , in [deg/s]) are shown in Fig. 6 (a) and (b), respectively. Based on these results, it is noted that the stabilization can be achieved by the quadcopter with the proposed AR marker detection technique-based image processing station. The basic control parameters of six PID controllers are based on results of the PID simulink simulation as shown in Fig. 3. It is observed that from the result graphs of Fig. 6 (a) and (b), the required settling-time to attain a stable attitude control mode of a quadcopter is about 17 seconds. After this time, the autonomous attitude control movement with the angular positions and angular speed parameters are successfully performed without aid of GPS under a real indoor environment.



(a)



(b)

**Figure 6:** Experimental results for tracking (a) three angular positions, and (b) three angular speeds of the quadcopter

### 5. Conclusion

This paper proposes the AR marker detection and image processing-based attitude control algorithm for a non-GPS aided quadcopter under the indoor environment. The AR marker detection technique is utilized in obtaining state information of the location and position of the quadcopter, which is carried out by detecting process of both green color AR marker and red color AR marker. Moreover, the dual closed loop control feedback PID controller with hierarchical (inner-loop and outer-loop) command update period are proposed for enhancing the reliability of the attitude and the position PID controllers. We presented experimental test results for demonstrating the quadrotor’s autonomous attitude control and operation in hovering under the real non-GPS aided indoor environment. The experiment results for tracking data of three angular positions and three angular speeds has shown that the stabilization can be achieved by the proposed autonomous attitude control strategy of the quadcopter. Therefore, the proposed mechanism with AR marker detection and the modified dual PID controllers is applicable to the GPS-denied indoor environments for autonomously navigating and hovering without external guidance or control.

### References

Achtelik, M., Bachrach, B. A., Ruijic, H., Samuel, P., & Nicholas, R. (2009). Autonomous navigation and exploration of a quadrotor helicopter in GPS-denied indoor environments. In *the First symposium on indoor flight*, 2009.  
 Anjum, A. S. K., Sufian, R. A., Abbas, Z., & Qureshi, I. M. (2016).

- Attitude Control of Quadcopter Using Adaptive Neuro Fuzzy Control. *International Journal of Hybrid Information Technology*, 9(4), 139–150.
- Cai, G., et al. (2014). A Survey of Small-Scale Unmanned Aerial Vehicles: Recent Advances and Future Development Trends. *Unmanned System Journal*, 2, 1–25.
- Elruby, A. Y., El-Khatib, M. M., El-Amary, N. H., & Hashad, A. I. (2012). Dynamic modeling and control of quadrotor vehicle. In *Proceedings of the 15th Int. AMME Conference* (Vol. 29, p. 31).
- Gheorghita, D., Vintu, I., Mirea, L., & Braescu, C. (2015). Quadcopter control system. In *IEEE 19th International Conference System Theory, Control and Computing (ICSTCC)*, 421–426.
- Goel, R., Shah, S. M., Gupta, N. K., & Ananthkrishnan, N. (2009). Modeling, simulation and flight testing of an autonomous quadrotor. In *Proceedings of ICEAE*, 1–7.
- Mian, A., & Wang, D. (2008). Modeling and Backstepping-based Nonlinear Control strategy for a 6 DOF Quadrotor Helicopter. *Chinese Journal of Aeronautics*, 21, 261–268.
- Nemati, A., & Kumar, M. (2014). Modeling and control of a single axis tilting quadcopter. In *IEEE 2014 American Control Conference (ACC)*, 3077–3082.
- Qi, J., Guan, X., & Lu, X. (2018). An Autonomous Pose Estimation Method of MAV Based on Monocular Camera and Visual Markers. In *2018 13th World Congress on Intelligent Control and Automation (WCICA)*, 252–257.
- Quach, C. H., Nguyen, D. H., Nguyen, V. T., Pham, M. T., & Phung, M. D. (2018). Real-time lane marker detection using template matching with RGB-D camera. In *IEEE 2nd International Conference on Recent Advances in Signal Processing, Telecommunications & Computing (SigTelCom)*, 152–157.
- Razinkova, A., Kang, B., Cho, H., & Jeon, H. (2014). Constant altitude flight control for quadrotor UAVs with dynamic feed-forward compensation. *International journal of fuzzy logic and intelligent systems*, 14(1), 26–33.
- Salih, A. L., Moghavvemi, M., Mohamed, H. A. F., & Gaeid, K. S. (2010). Flight PID controller design for a UAV quadrotor. *Scientific Research and Essays*, 5(23), 3660–3667.
- Seidabad, E. A., et al. (2014). Designing Fuzzy PID Controller for Quadrotor. *International Journal of Advanced Research in Computer Science and Technology*, 2, 221–227.
- Tahir, Z., Jamil, M., Liaqat, S. A., Mubarak, L., Tahir, W., & Gilani, S. O. (2016). Design and development of optimal control system for quadcopter UAV. *Indian Journal of Science and Technology*, 9(25).